British Journal of Pharmacology

British Journal of Pharmacology (2019) **176** 725–736 725

RESEARCH PAPER

Acute effects of zinc and insulin on arcuate anorexigenic proopiomelanocortin neurons

Correspondence Kevin W. Williams, Division of Hypothalamic Research, The University of Texas Southwestern Medical Center at Dallas, 5323 Harry Hines Boulevard, Dallas, TX 75390-9077, USA. E-mail: kevin.williams@utsouthwestern.edu

Received 12 June 2018; **Revised** 15 November 2018; **Accepted** 24 November 2018

Zhenyan He[1,3,*], Yong Gao[2,3,*], Linh Lieu[3], Sadia Afrin[3], Hongbo Guo[1,†] and Kevin W Williams[3,†]

[1]The National Key Clinical Specialty, The Engineering Technology Research Center of Education Ministry of China, Guangdong Provincial Key Laboratory on Brain Function Repair and Regeneration, Department of Neurosurgery, Zhujiang Hospital, Southern Medical University, Guangzhou, China, [2]National Laboratory of Medical Molecular Biology, Institute of Basic Medical Sciences, Chinese Academy of Medical Sciences and Peking Union Medical College, Beijing, China, and [3]Division of Hypothalamic Research, Department of Internal Medicine, The University of Texas Southwestern Medical Center at Dallas, Dallas, TX USA

*These authors are co-first authors.
†These authors are co-corresponding authors.

BACKGROUND AND PURPOSE

Acute insulin administration hyperpolarized, with concomitant decrease of firing rate, a subpopulation of arcuate proopiomelanocortin (POMC) and neuropeptide Y/agouti-related peptide cells. This rapid effect on cellular activity has been proposed as a cellular correlate of insulin effects on energy balance and glucose homoeostasis. Recent evidence suggests that zinc in mammalian insulin formulations is required for the insulin-induced inhibition of arcuate POMC neurons, while guinea pig insulin, which fails to bind zinc, activates POMC neurons in mice. Here, we tested the effects of zinc and insulin formations on arcuate POMC neurons.

EXPERIMENTAL APPROACH

Effects of zinc and insulin formulations were assessed through whole-cell patch clamp recordings on transgenic mice *in vitro*.

KEY RESULTS

Insulin formulations containing zinc hyperpolarized POMC neurons. Zinc also hyperpolarized arcuate POMC neurons, albeit at much higher concentration than found in various insulin formulations. Chelation of zinc inhibited the zinc-induced hyperpolarization of POMC neurons, whereas effects of insulin on POMC cellular activity were unchanged after chelation. Zinc-free insulin also hyperpolarized arcuate POMC neurons. Insulin failed to hyperpolarize POMC neurons deficient for insulin receptors, suggesting that insulin receptors are required for these effects. Activation of POMC neurons by guinea pig insulin was independent of insulin receptors but was inhibited by PDGF receptor antagonism or loss of TRPC5 channel subunits.

CONCLUSIONS AND IMPLICATIONS

Together, these findings suggest that insulin inhibited arcuate POMC neurons independent of zinc and highlights a possible role of putative PDGF receptors in the acute effects of guinea pig insulin.

Abbreviations

AgRP, agouti-related peptide; NPY, neuropeptide Y; POMC, proopiomelanocortin

DOI:10.1111/bph.14559

WHAT IS ALREADY KNOWN

- Zinc inhibited arcuate proopiomelanocortin (POMC) neurons.
- Insulin formulations (with zinc) inhibited arcuate POMC neurons.
- Guinea pig insulin activated arcuate POMC neurons.

WHAT THIS STUDY ADDS

- Zinc-free insulin inhibited arcuate POMC neurons independent of zinc.
- Zinc concentration in insulin formulations is not sufficient to alter arcuate POMC neurons.
- Guinea pig insulin activated POMC neurons *via* putative PDGF receptors and TRPC5 channel subunits, independent of insulin receptors.

WHAT IS THE CLINICAL SIGNIFICANCE

- The current study confirms that the acute effect of insulin in arcuate POMC neurons is predominantly inhibitory.
- The current study demonstrates that the acute effects of guinea pig insulin on arcuate POMC and neuropeptide Y neurons are independent of insulin receptors.

Introduction

Insulin receptors within the brain have been directly linked to energy balance and glucose homoeostasis (Woods *et al.*, 1979; Bruning *et al.*, 2000; Plum *et al.*, 2005). Proopiomelanocortin (**POMC**) and neuropeptide Y/agouti-related peptide (**NPY**/**AgRP**) neurons within the hypothalamic arcuate nucleus are common nodes for these activities. Importantly, acute activation of both POMC and NPY/AgRP neurons is sufficient to alter feeding behaviour and glucose metabolism (Aponte *et al.*, 2011; Krashes *et al.*, 2011; Steculorum *et al.*, 2016). While many of the pleiotropic effects of **insulin** have been attributed to cell signalling which might alter gene regulation, recent work has highlighted a role for insulin in modifying acute neuronal activity resulting in measurable metabolic outcomes (Plum *et al.*, 2006; Steculorum *et al.*, 2016). In particular, insulin inhibits POMC neurons *via* activation of $\mathbf{K_{ATP}}$ channels, acting to suppress hepatic glucose production (Plum *et al.*, 2006; Hill *et al.*, 2008; Williams *et al.*, 2010). However, recent work suggests that this activity might be confounded by the presence of **zinc** in various mammalian insulin formulations (Qiu *et al.*, 2014, 2018). Moreover, hystricomorph insulin (putative zinc-free insulin) activates arcuate POMC neurons *via* a mixed-cation channel, putative **TRPC** channel conductance (Qiu *et al.*, 2014, 2018). While these data suggest that zinc in insulin formulations may contribute to altered cellular properties, the role of zinc in various insulin formulations to alter cellular activity has not been examined. Recent evidence suggests that **TRPC5** channel subunits are important regulators of POMC cellular activity in response to several metabolic signals (Gao *et al.*, 2017). However, the requirement of specific TRPC channel subunits in the activation of arcuate POMC neurons induced by guinea pig insulin, remains unknown.

In the current study, the hypothesis that non-hystricomorph insulin inhibits arcuate POMC and NPY neurons independent of zinc was tested using whole-cell patch-clamp electrophysiology in acute hypothalamic slices from transgenic mice. Acute effects of zinc, zinc-containing insulin, zinc-free insulin and guinea pig insulin were assessed on intrinsic membrane properties of arcuate POMC and NPY neurons, including subsets of neurons which express or do not express leptin receptors. The requirement of TRPC5 channel subunits in the acute effects of guinea pig insulin to depolarize POMC neurons was also examined.

Methods

Animal care

All animal care and experimental procedures complied with the guidelines established by the National Institute of Health Guide for the Care and Use of Laboratory Animals and were approved by the University of Texas Institutional Animal Care and Use Committee. Animal studies are reported in compliance with the ARRIVE guidelines (Kilkenny *et al.*, 2010).

The 7–9 weeks pathogen-free male POMC-hrGFP::LepR-cre::td-tomato (POMC-hrGFP mice RRID: IMSR_JAX:006421; LepR-cre mice RRID: IMSR_JAX:008320; td-tomato mice RRID: IMSR_JAX:007908) (He *et al.*, 2018; Huang *et al.*, 2018; Sohn and Williams, 2012; Williams *et al.*, 2014), POMC-hrGFP::LepR-cre::td-tomato::TRPC5 KO (TRPC5 KO mice RRID: IMSR_JAX:030804) (Gao *et al.*, 2017), POMC-creER::IR-flox::LepR-flox::td-tomato (POMC-CreER^{t2} mice RRID: MGI: 5569339, IR-flox mice RRID: IMSR_JAX:006955, LpeR-flox mice RRID: IMSR_JAX:018989) and NPY-hrGFP mice (NPY-hrGFP mice RRID: IMSR_JAX:006417) (Sun *et al.*, 2016) were used for all experiments. All mice were housed under standard laboratory conditions (12 h on/off; lights on at 7:00 a.m.) and temperature-controlled environment. All mice were provided a Harlan Teklad 2016 chow diet and water *ad libitum* unless otherwise noted. The number of mice in each experiment groups in this study is shown in the Figure legends.

Tamoxifen treatment to induce adult-onset ablation of both insulin receptors and leptin receptors in POMC neurons

Tamoxifen (Sigma, 20 mg·mL^{-1}) dissolved in corn oil (Sigma) was administered i.p. for 2 consecutive days (80 μL·day^{-1}) to 5- to 7-week-old male POMC-creER::IR-flox::LepR-flox::td-tomato mice. Moist food was provided after the injection of tamoxifen. After 2 weeks of injection, mice were used for electrophysiology recording.

Electrophysiology studies

Slice preparation and whole-cell recordings. Brain slices were prepared from young adult male mice (7–9 weeks old) as previously described (Sohn and Williams, 2012; Williams *et al*., 2014; Sun *et al*., 2016; Gao *et al*., 2017). Briefly, male mice were deeply anaesthetized with 7% chloral hydrate (i.p.) and transcardially perfused with a modified ice-cold artificial CSF (ACSF) (described below). The mice were then decapitated, and the entire brain was removed and immediately submerged in ice-cold, carbogen-saturated (95% O2 and 5% CO2) ACSF (126 mM NaCl, 2.8 mM KCl, 1.2 mM MgCl2, 2.5 mM CaCl2, 1.25 mM NaH2PO4, 26 mM NaHCO3 and 5 mM glucose). Coronal sections (250 μm) were cut with a Leica VT1000S Vibratome and then incubated in oxygenated ACSF at room temperature for at least 1 h before recording. The slices were bathed in oxygenated ACSF (32–34°C) at a flow rate of ~2 mL·min^{-1}. All electrophysiology recordings were performed at room temperature.

After an equilibration period of 1–2 h, whole-cell patch-clamp recordings were obtained from POMC and NPY neurons in the arcuate nucleus using patch pipettes with open tip resistance of 2–5 MΩ. Seal resistance was 1–5 GΩ, and series resistance was <24 MΩ, uncompensated. The pipette solution for whole-cell recording was modified to include an intracellular dye (Alexa Fluor 350 hydrazide dye) for whole-cell recording: 120 mM K-gluconate, 10 mM KCl, 10 mM HEPES, 5 mM EGTA, 1 mM CaCl2, 1 mM MgCl2 and 2 mM MgATP, 0.03 mM Alexa Fluor 350 hydrazide dye (pH 7.3). Epifluorescence was briefly used to target fluorescent cells, after which the light source was switched to infrared differential interference contrast imaging to obtain the whole-cell recording (Zeiss Axioskop FS2 Plus equipped with a fixed stage and a QuantEM:512SC electron-multiplying charge-coupled device camera). Electrophysiological signals were recorded using an Axopatch 700B amplifier (Molecular Devices), low-pass filtered at 2–5 kHz and analysed offline on a PC with pCLAMP programs (pClamp, Ver 10.4, RRID: SCR_011323, Molecular Devices). Membrane potential and firing rate were measured by whole-cell current-clamp recordings from POMC and NPY neurons in brain slices. Recording electrodes had resistances of 2.5–5 MΩ when filled with the K-gluconate internal solution. Input resistance was assessed by measuring voltage deflection at the end of the response to a hyperpolarizing rectangular current pulse steps (500 ms of −10 to −50 pA).

Solutions containing drug were typically perfused for 5 min. A drug effect was required to be associated temporally with compound application, and the response had to be stable within a few minutes. A change in membrane potential was required to be at least 2 mV in amplitude; the onset was required to be associated temporally with the peptide application (i.e. usually beginning at about 1–2 min after changing solutions, the time it took for compound to arrive at the recording chamber), and the response had to be saturated and stable within a few minutes (i.e. did not continually change) and had to be reversible or partially reversible upon washout of the drug. The value of the membrane potential was measured at a specific time after compound application (i.e. 3–4 min after the compound arrived in the chamber and no continual changes).

Data and statistical analysis

The data and statistical analysis in this study comply with the recommendations of the British Journal of Pharmacology on experimental design and analysis in pharmacology. No blinding or randomization was undertaken in this study. It is not a usual procedure for this form of study and cannot be applied retrospectively. No normalization was undertaken in this study. All data are given as mean ± SEM from the indicated number (*n*) of independent experiments. Cell numbers studied for different groups are designed to be equal. Data points were excluded if the baselines were unstable or if the resistance changed before the experiment concluded, which has resulted in different group numbers for some experiments. Membrane potential values were not compensated to account for junction potential (−8 mV). All graphs were carried out using GraphPad Prism 7.0 software (GraphPad Prism, Ver 7.0, RRID: SCR_002798). All figures were carried out using CorelDraw C8 (64 bit).

Materials

Production of zinc-free insulin. Biosynthetic human insulin zinc crystals (110 mg) were solubilized in 16 mM HCl. The insulin was loaded on a reversed phase column (C8, 10 micron, 150 × 10 mm I.D., YMC) and eluted with a gradient of 10 to 50% acetonitrile over six column volumes. Tris and EDTA were added to the reversed phase pool to final concentrations of 20 and 5 mM, respectively, and the pH was adjusted to 7.6. The sample was dialysed against water using a 2000 Dalton cut-off regenerated cellulose membrane. After dialysis, the pH was adjusted from 6.8 to 7.4, and the volume was adjusted with water to a final insulin concentration of 94.9 μM (determined by analytical reversed phase HPLC). The final zinc content was determined by ICP-MS to be 1 zinc ion for every 3300 insulin molecules. The final sample was stored at −20°C in 0.1 mL aliquots.

Zinc chloride (0.05–10 μM, Sigma, dissolved in water), Humulin-R (50 nM, Eli Lilly), Sigma insulin (50 nM, Sigma), zinc-free insulin (1–500 nM, Eli Lilly), guinea pig insulin (50 nM, National Hormone and Peptide Program, Harbor-UCLA Medical Center, dissolved in water), **leptin** (100 nM, provided by A.F. Parlow, through the National Hormone and Peptide Program, dissolved in PBS), EDTA (micromolar concentrations of EDTA were combined with zinc or insulin and resulted a final concentration of 450 nM EDTA in perfusion chamber; Sigma, dissolved in water) and CP 673451 (100 nM, Tocris, dissolved in ethanol) were added to the ACSF for specific experiments.

Nomenclature of targets and ligands

Key protein targets and ligands in this article are hyperlinked to corresponding entries in http://www.guidetopharmacology.org, the common portal for data from the IUPHAR/BPS Guide to PHARMACOLOGY(Harding *et al.*, 2018), and are permanently archived in the Concise Guide to PHARMACOLOGY 2017/18 (Alexander *et al.*, 2017a,b,c,d).

Results

Insulin hyperpolarized POMC neurons in arcuate nucleus of the hypothalamus independent of zinc

Arcuate POMC neurons were targeted in POMC-hrGFP mice (Figure 1A–D) for whole-cell patch-clamp recordings. Similar to a previous report (Qiu *et al.*, 2014), zinc dose-dependently hyperpolarized arcuate POMC neurons from POMC-hrGFP mice (0.05–5 μM, EC_{50} = 0.4 μM, n = 39, Figure 1E,J). The hyperpolarization was concomitant with a decrease in input resistance (16.4%, n = 3, 0.8 ± 0.1 GΩ for control; 0.67 ± 0.07 GΩ for zinc, Figure 1F,G). Subsequent linear regression analysis revealed the reversal potential of the zinc-induced hyperpolarization to be −98 ± 1.5 mV (Figure 1F). Thus, similar to previous reports of insulin in arcuate POMC neurons (Plum *et al.*, 2006; Williams *et al.*, 2010, 2014), these data support a zinc-dependent activation of a putative potassium conductance.

In order to determine if zinc is contributing to the hyperpolarization of arcuate POMC neurons in response to insulin, we first attempted to sequester free zinc in various insulin formulations using the chelating agent EDTA. As a proof of principle, we utilized a dose of EDTA that failed to alter the membrane potential of arcuate POMC neurons (EDTA = 450 nM; Figure 1H). Notably, pretreatment with EDTA blunted the dose-dependent hyperpolarization of POMC neurons induced by zinc (0.1–10 μM, EC_{50} = 3 μM, n = 50, Figure 1I,J). Thus, if the previously described insulin-induced hyperpolarization of arcuate POMC neurons required zinc, then EDTA should similarly cause a rightward shift in the response.

Next, we examined the effect of EDTA on the insulin-induced inhibition of arcuate POMC neurons. Recent data suggest that the acute effects of insulin and leptin on arcuate POMC neurons were largely segregated (Williams *et al.*, 2010, 2014); therefore, we targeted POMC neurons which do not express leptin receptors (Figure 2A–E) for whole-cell patch-clamp recordings. Consistent with previous reports (Plum *et al.*, 2006; Hill *et al.*, 2008; Williams *et al.*, 2010), five out of six POMC neurons which did not express leptin receptors were hyperpolarized by −7.4 ± 1.4 mV in response to insulin (50 nM, Humulin-R; n = 5, Figure 2F,J). Similarly, five out of seven POMC neurons which did not express leptin receptors were hyperpolarized by −7.0 ± 0.5 mV in response to insulin (50 nM, Sigma insulin, n = 5, Figure 2H,J). Notably, the insulin-induced hyperpolarization of POMC neurons which did not express leptin receptors persisted after pretreatment with EDTA (−7.2 ± 0.8 mV, n = 4, Humulin-R; −7.4 ± 2.1 mV, n = 4, Sigma insulin, Figure 2G,I,J). In order to further assess if the insulin-induced effect on POMC neurons was dependent on zinc, we obtained a zinc-free insulin formulation (Eli Lilly). Notably, the hyperpolarization induced by zinc-free insulin (1–500 nM, EC_{50} = 100 nM, n = 41, Figure 2K,L) was analogous to that of the commercially available insulin. We also examined the effect of leptin on POMC neurons following pretreatment with 450 nM EDTA. As observed with insulin, the leptin-induced depolarization of POMC neurons which express leptin receptors persisted after pretreatment with EDTA (Supporting Information Figure S1). Together, these data suggest that pretreatment with EDTA appeared to selectively chelate zinc, blocking the effects of zinc on POMC neurons, independent of altering other divalent cations or activity of ion channels.

We then examined the effects of insulin on the membrane potential of arcuate NPY neurons (Supporting Information Figure S2A–D). Recent work suggests that the acute effects of insulin are widespread in NPY neurons (Huang *et al.*, 2018). In particular, NPY neurons were inhibited by insulin, regardless of their neurons expressing leptin protein (Huang *et al.*, 2018). Consistent with previous reports (Huang *et al.*, 2018; Xu *et al.*, 2018), 9 of 13 NPY neurons from NPY-hrGFP mice were hyperpolarized by −9.7 ± 0.9 mV in response to insulin (50 nM, Humulin-R, Supporting Information Figure S2E,I) and four of seven NPY neurons were hyperpolarized by −11.9 ± 0.02 mV in response to insulin (50 nM, Sigma insulin, Supporting Information Figure S2G,I). Pretreatment with EDTA failed to inhibit the insulin-induced hyperpolarization of NPY neurons (50 nM, Humulin-R, −14.8 ± 3.0 mV, n = 5, Supporting Information Figure S2F,I; 50 nM, Sigma insulin, −12.6 ± 1.4 mV, n = 5, Supporting Information Figure S2H,I). Together, these data suggest that insulin hyperpolarized both POMC and NPY neurons, independent of the activity of zinc.

Guinea pig insulin depolarized arcuate POMC neurons via TRPC5 channels

Guinea pig insulin activates arcuate POMC neurons (Figure 3F). In particular, four out of nine POMC neurons expressing leptin receptors (Figure 3A–E) were depolarized in response to guinea pig insulin (44.4%, 11 ± 1.4 mV, n = 4, Figure 3G), whereas 1 out of 12 POMC neurons which do not express leptin receptors (Figure 2A–E) was depolarized in response to guinea pig insulin (8.3%, 10.2 mV, n = 1, Figure 3G). Analysis of current–voltage relationships suggests that guinea pig insulin decreased input resistance of arcuate POMC neurons (n = 3, from 1.2 ± 0.17 GΩ in control ACSF to 0.9 ± 0.17 GΩ in guinea pig insulin), with a reversal potential of −8.1 ± 3.9 mV (n = 3, Figure 4H,I). In a similar manner to leptin (Hill *et al.*, 2008; Williams *et al.*, 2010; Gao *et al.*, 2017), guinea pig insulin activated a non-selective cation conductance which depolarized arcuate POMC neurons predominantly expressing leptin receptors.

TRPC5 channel subunits are required for the leptin-induced activation of POMC neurons (Gao *et al.*, 2017). As guinea pig insulin and leptin share a similar mechanism of action to activate a non-selective cation channel in POMC neurons expressing leptin receptors, we hypothesized that

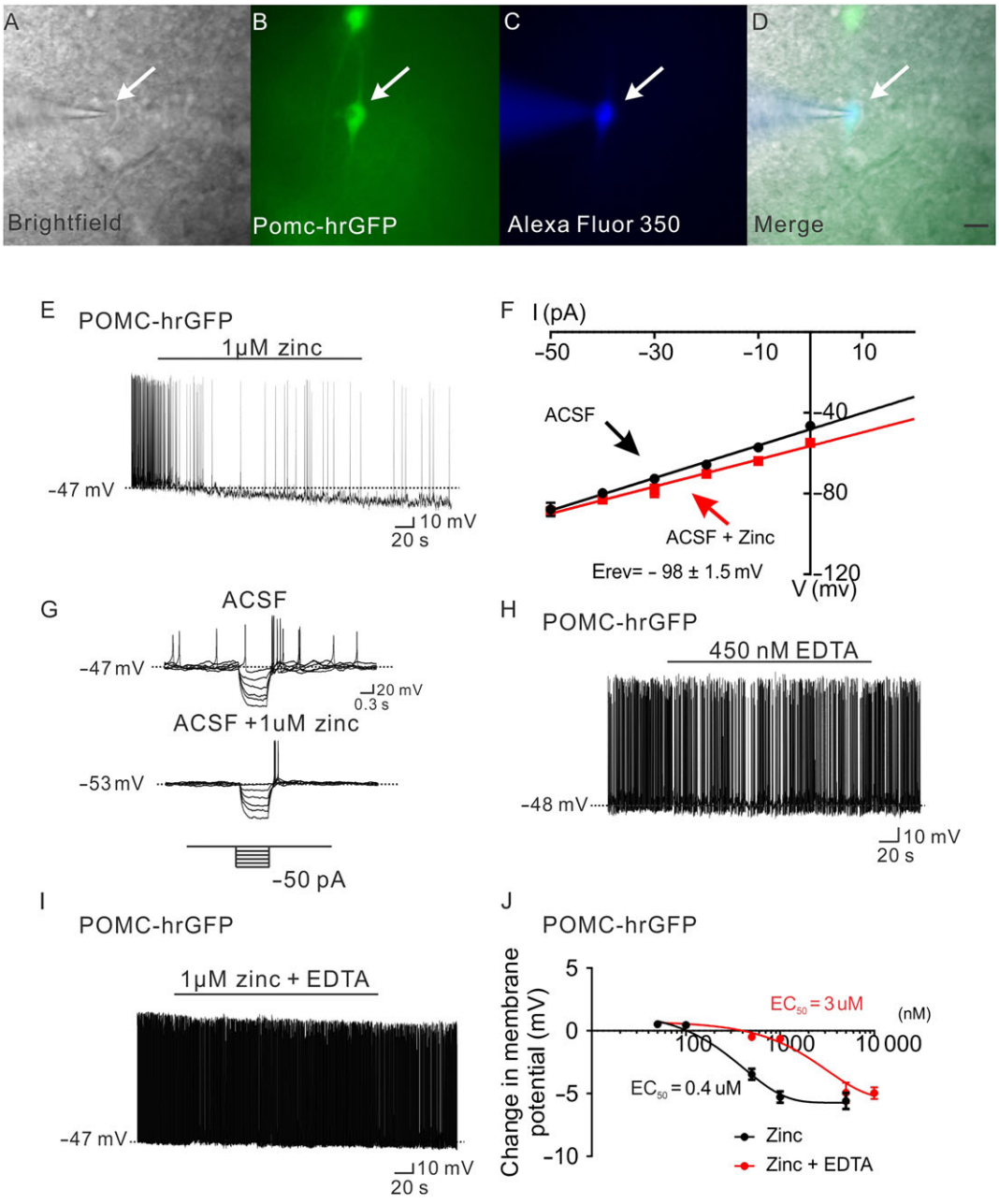

Figure 1

Zinc hyperpolarizes POMC neurons in the arcuate nucleus of hypothalamus. (A–D) Brightfield illumination (A) of POMC neuron from POMC-hrGFP mice. (B) Shows the same neuron under FITC (hrGFP) illumination. Complete dialysis of Alexa Fluor 350 from the intracellular pipette is shown in (C) and merged image of targeted POMC neuron (D). Arrow indicates the targeted cell. Scale bar = 50 μm. (E) Current-clamp recording demonstrates that administration of zinc (1 μM) hyperpolarized POMC neurons. (F) Current versus voltage (I–V) relationship for the group of POMC neurons examined in response to zinc (1 μM). (G) Current-clamp recording from a POMC neuron showing a decreased voltage deflection in response to current injection after zinc application. (H,I) Application of EDTA has no effect on the membrane potential of POMC neurons, and administration of EDTA blunted zinc (1 μM) induced hyperpolarization of POMC neurons. (J) Dose-response to zinc and zinc + EDTA on POMC neurons. (zinc: n = 39; zinc + EDTA: n = 50. Data from 21 mice.)

guinea pig insulin may also mediate its excitatory effects *via* TRPC5 channel subunits. POMC neurons from mice deficient for TRPC5 channel subunits were used for electrophysiological recordings (POMC-hrGFP::LepR-icre:: td-tomato mice::TRPC5 KO; Gao *et al.*, 2017). Application of guinea pig insulin (50 nM) failed to depolarize POMC neurons (regardless of the expression of leptin receptors) from mice deficient in TRPC5 channel subunits (change of resting membrane potential: −0.2 ± 0.7 mV, n = 12, Figure 3J,K), supporting a requirement of these channel

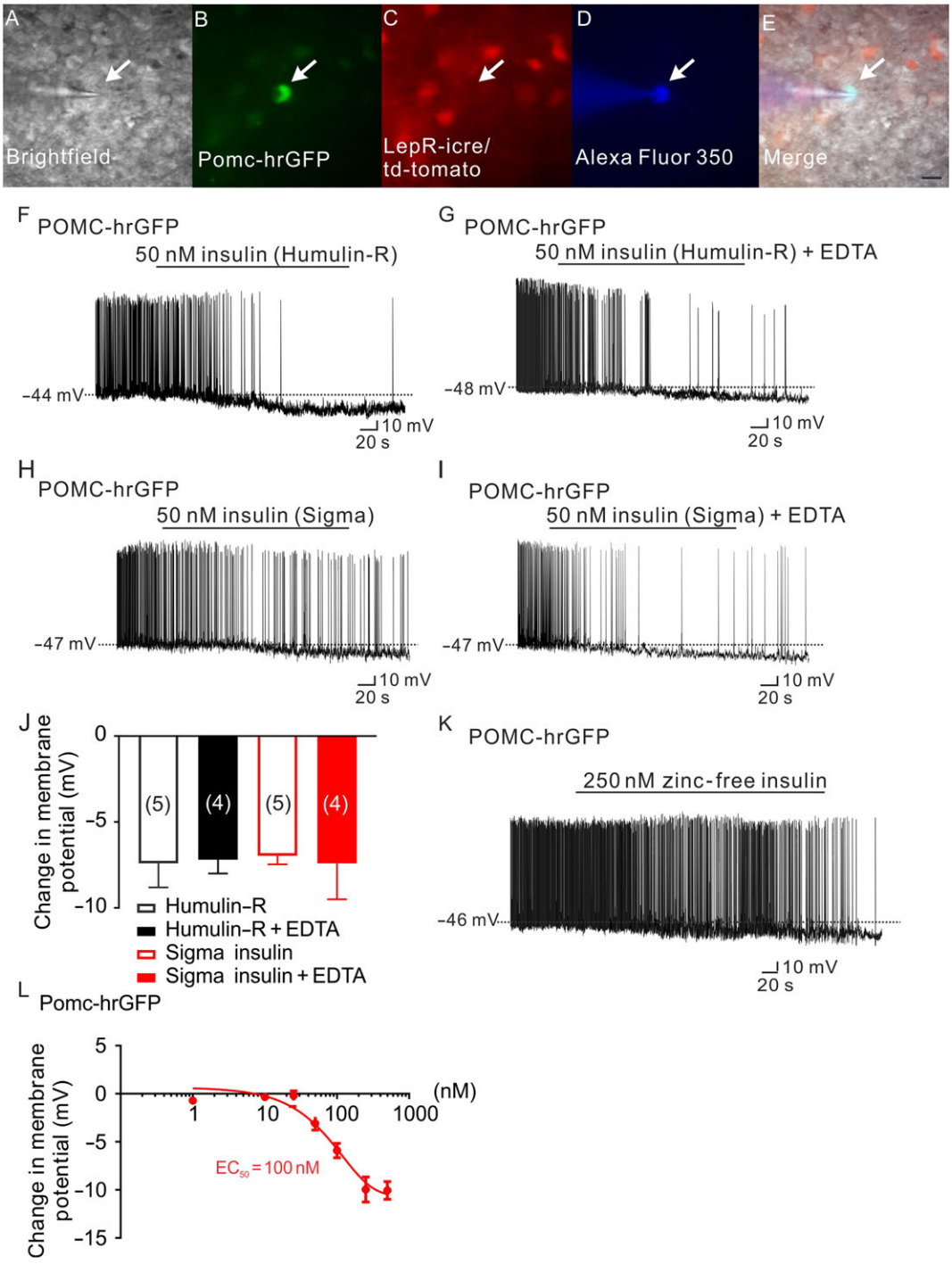

Figure 2

Insulin hyperpolarizes arcuate POMC neurons independent of zinc. (A–E) Brightfield illumination (A) of a POMC neuron that does not express leptin receptors from POMC-hrGFP::LepR-cre::td-tomato mice. (B) and (C) show the same neuron under FITC (hrGFP, green cell) and Alexa Fluor 594 (td-tomato, not red cell) illumination. Complete dialysis of Alexa Fluor 350 from the intracellular pipette is shown in (D) and merged image of a POMC neuron targeted for electrophysiological recording (E). (Arrow indicates the targeted cell. Scale bar = 50 μm). (F,H) Representative traces depicting a POMC neuron hyperpolarized by insulin (50 nM, Humulin-R; F) and insulin (50 nM, Sigma insulin; H). (G,I) Administration of EDTA does not block either the Humulin-R (50 nM) or the Sigma insulin (50 nM) induced hyperpolarization of POMC neurons. (J) Histogram illustrates the acute effects of insulin on the membrane potential of POMC neurons with or without EDTA. Error bars indicate SEM. (Humulin-R: $n = 6$; Humulin-R + EDTA: $n = 7$; Sigma insulin: $n = 7$; Sigma insulin: $n = 7$. Data from 11 mice.) (K) Representative traces showing that POMC neurons are hyperpolarized by zinc-free insulin (250 nM). (L) Dose-response of zinc-free insulin on POMC neurons. ($n = 41$. Data from 13 mice.)

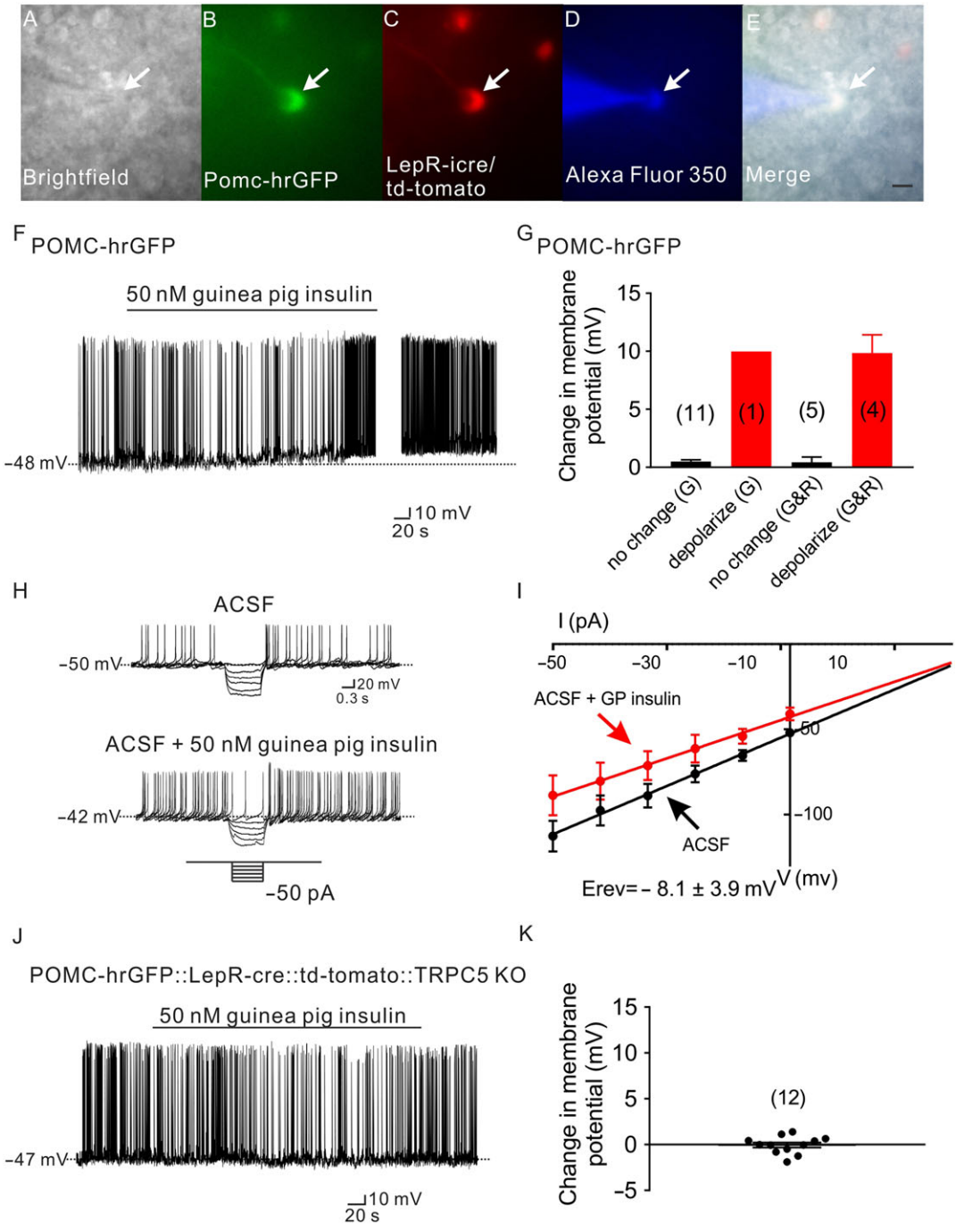

Figure 3

Guinea pig insulin depolarizes arcuate POMC neurons *via* TRPC5 channel subunits. (A–E) Brightfield illumination (A) of POMC neurons that expresses leptin receptors from POMC-hrGFP::LepR-cre::td-tomato mice. (B) and (C) show the same neuron under FITC (hrGFP, green cell) and Alexa Fluor 594 (td-tomato, red cell) illumination. Complete dialysis of Alexa Fluor 350 from the intracellular pipette is shown in (D) and merged image of targeted POMC neuron (E). Arrow indicates the targeted cell. Scale bar = 50 μm. (F) Representative current-clamp trace depicts that a POMC neuron is depolarized by guinea pig insulin (50 nM). (G) Histogram illustrates guinea pig insulin-induced changes in the membrane potential of POMC neurons. G: POMC neuron which does not express leptin receptors. G&R: POMC neuron which expresses leptin receptors. Error bars indicate SEM. (G: $n = 12$; G&R: $n = 9$. Data from seven mice.) (H) Current-clamp recording from a POMC neuron showing a decreased voltage deflection in response to current injection after guinea pig insulin application (50 nM). (I) Current versus voltage (I–V) relationship for the group of POMC neurons examined in response to guinea pig insulin. (J) Representative trace shows that POMC neurons which express LepRs and are deficient for TRPC5 subunits from POMC-hrGFP::LepR-cre::td-tomato::TRPC5 KO mice fail to alter the membrane potential in response to guinea pig insulin (50 nM). (K) Histogram illustrates guinea pig insulin-induced change of membrane potential of POMC neurons from POMC-hrGFP::LepR-cre::td-tomato::TRPC5 KO mice. Error bars indicate SEM ($n = 12$. Data from four mice.)

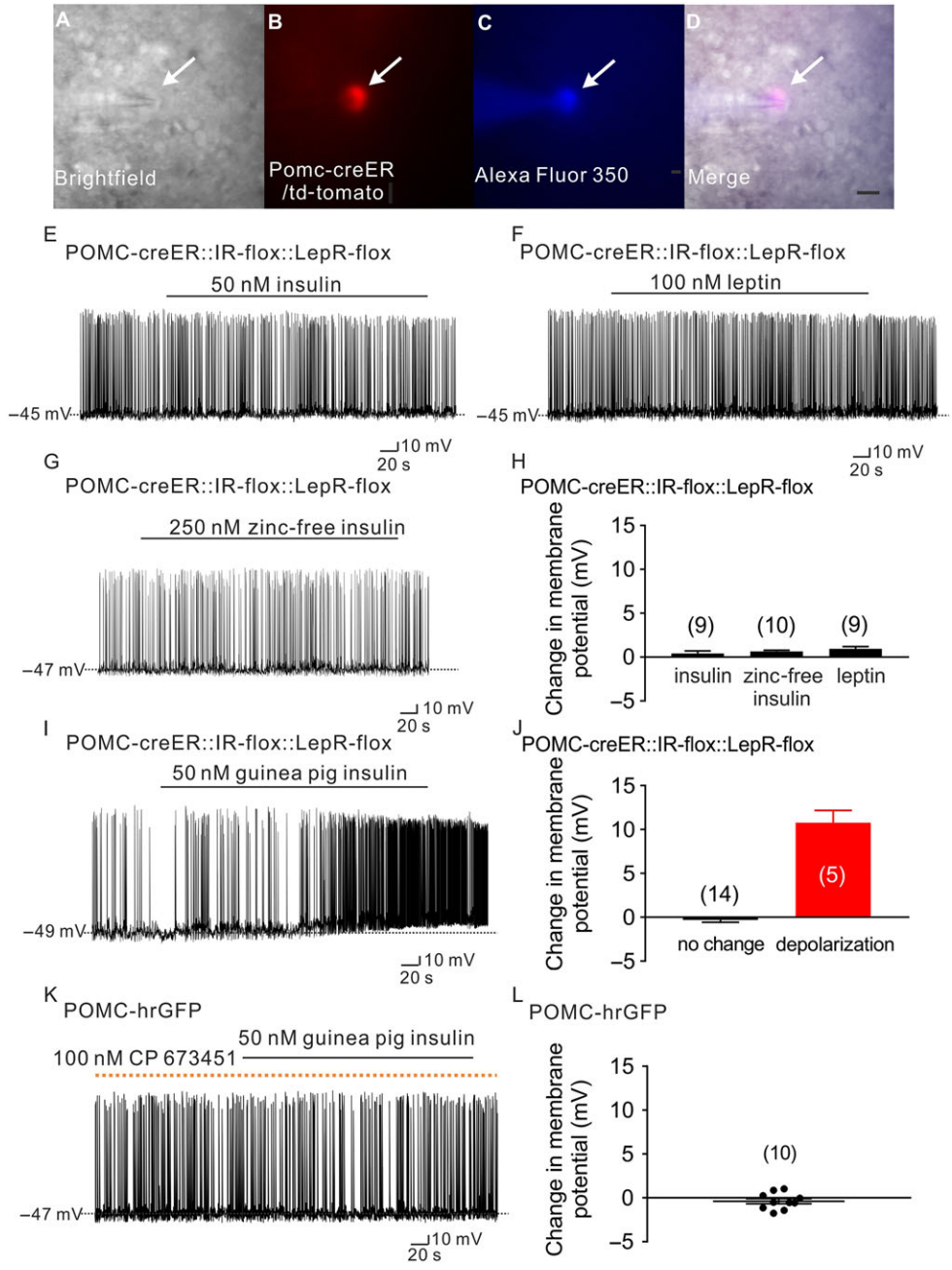

Figure 4

Guinea pig insulin activates arcuate POMC neurons dependent on PDGF receptors, independent of leptin receptors or insulin receptors. (A–D) Brightfield illumination (A) of POMC neuron from POMC-creER::IR-flox::LepR-flox::td-tomato mice. (B) Shows the same neuron under TRITC (td-tomato) illumination. Complete dialysis of Alexa Fluor 350 from the intracellular pipette is shown in (C) and merged image of targeted POMC neuron (D). Arrow indicates the targeted cell. Scale bar = 50 μm. (E–G) Current-clamp record demonstrates that insulin (50 nM, Humulin-R), leptin (100 nM) and zinc-free insulin (250 nM) fail to alter the cellular excitability of POMC neurons deficient for leptin receptors and insulin receptors from POMC-creER::IR-flox::LepR-flox::td-tomato mice. (H) Histogram illustrates insulin- and leptin-induced changes of membrane potential of POMC neurons from POMC-creER::IR-flox::LepR-flox::td-tomato mice. Data shown are means ± SEM from 10 mice; insulin: $n = 9$; zinc-free insulin: $n = 10$; leptin: $n = 9$, they have added 10 mice). (I) A representative trace shows that POMC neurons which are deficient for leptin receptors and insulin receptors are depolarized by guinea pig insulin (50 nM). (J) Histogram illustrates guinea pig insulin-induced change of membrane potential of POMC neurons from POMC-creER::IR-flox::LepR-flox::td-tomato mice. Error bars indicate SEM; $n = 19$; data from six mice. (K) A representative trace demonstrates that pretreatment with the PDGF receptor antagonist, CP 673451, prevents the guinea pig insulin (50 nM) induced depolarization of POMC neurons. Dotted line: treatment of CP 673451. (L) Histogram illustrates guinea pig insulin-induced change of membrane potential of POMC neurons after pretreatment with CP 673451. Values shown are means with SEM; $n = 10$; data from four mice.)

subunits in the excitation of arcuate POMC neurons, induced by guinea pig insulin.

Guinea pig insulin activated arcuate POMC neurons via PDGF receptors, independent of insulin receptors and leptin receptors

Guinea pig insulin may have promiscuous trophic properties in mammalian systems (King *et al*., 1983; Chan *et al*., 1984). In order to better determine the requirement of insulin receptors or leptin receptors in the activation of POMC neurons induced by guinea pig insulin, we generated mice deficient in both insulin receptors and leptin receptors in adult POMC neurons. In particular, POMC reporter mice were first generated by mating POMC-creER^{T2} mice (Berglund *et al*., 2013) with the td-tomato reporter mouse (Jackson Laboratory, #007908). POMC-creER^{T2}::td-tomato reporter mice were subsequently mated to both InsR-lox (Bruning *et al*., 1998) and LepR-lox (Balthasar *et al*., 2004) mice to generate POMC reporter mice deficient for both insulin receptors and leptin receptors in POMC neurons (POMC-creER::InsR-flox::LepR-flox::td-tomato mice). As expected, zinc-containing insulin (50 nM, Humulin-R), zinc-free insulin (250 nM) and leptin (100 nM) all failed to alter the membrane potential of these POMC neurons (Figure 4A–D), deficient in insulin receptors and leptin receptors (Humulin-R: change of resting membrane potential: 0.4 ± 0.3 mV, n = 9; zinc-free insulin: change of resting membrane potential: 0.6 ± 0.1 mV, n = 10; and leptin: change of resting membrane potential: 0.9 ± 0.2 mV, n = 9, Figure 4E–H). However, the guinea pig insulin-induced depolarization of POMC neurons persisted in POMC neurons deficient for both insulin receptors and leptin receptors (26.3%, 10.5 ± 1.4 mV, n = 5, Figure 4I–J). The remaining 14 cells (73.7%) were not responsive to guinea pig insulin (−0.3 ± 0.3 mV, n = 14, Figure 4J). Importantly, the percentage of cells responding to guinea pig insulin in POMC neurons deficient in insulin receptors and leptin receptors (26.3%) was similar to that in wild-type POMC neurons (23.8%).

In agreement with results suggesting that guinea pig insulin shares biological activity with **PDGF receptors**, guinea pig insulin failed to depolarize arcuate POMC neurons after pretreatment with the selective PDGF receptor antagonist (100 nM CP 673451: change of resting membrane potential: −0.4 ± 0.3 mV, n = 10, Figure 4K,L). Notably, CP 673451 (100 nM) failed to block the hyperpolarization of POMC neurons induced by insulin (50 nM, Humulin-R, Eli Lilly) (Supporting Information Figure S3). These data support an acute activity of guinea pig insulin in arcuate POMC neurons *via* putative PDGF receptors.

We also made electrophysiological recordings from NPY neurons in the presence of guinea pig insulin. Similar to previous reports (Qiu *et al*., 2014), guinea pig insulin (50 nM) inhibited arcuate NPY neurons resulting in a decrease in excitability (Supporting Information Figure S4). Moreover, the effects of guinea pig insulin on arcuate NPY neurons were blocked by the PDGF receptor antagonist (100 nM CP 673451; Supporting Information Figure S5).

Together, these data suggest that insulin (zinc containing and zinc-free) and leptin act on POMC neurons *via* insulin receptors and leptin receptors respectively. In contrast, the guinea pig insulin-induced activation of POMC neurons and inhibition of NPY neurons required putative PDGF receptors, but was independent of both insulin receptors and leptin receptors.

Discussion

Zinc-containing and zinc-free insulin formulations hyperpolarized arcuate POMC neurons *via* insulin receptors. Conversely, guinea pig insulin depolarized arcuate POMC neurons *via* PDGF receptors and TRPC5 channel subunits, independent of insulin receptors and leptin receptors. These findings highlight insulin's inhibitory effect on arcuate POMC neurons and suggest a possible mechanism for how guinea pig insulin excites POMC neurons independent of insulin receptors and LepRs. (Summarized in Supporting Information Figure S6.)

Effects of zinc and zinc-free insulin on arcuate POMC neuronal excitability

Recent work suggests that commercial insulin products (which contain zinc) hyperpolarize arcuate POMC neurons *via* a zinc-dependent activation of an ATP-sensitive potassium channel while in the absence of zinc, insulin excites arcuate POMC neurons (Qiu *et al*., 2014). However, current models have not fully examined the effects of zinc (within these insulin formulations) and zinc-free insulin to induce acute effects on POMC neuronal activity. It should also be noted that recent work suggested commercial formulations of insulin (bovine insulin: Sigma I-1882 and human insulin: Sigma I-9278) were 'unadulterated' or zinc-free (Qiu *et al*., 2014). In fact, these insulin formulations contain concentrations of zinc equal to or greater than other insulin formulations (including Humulin-R and Novolin; personal communication with Sigma). However, instead of observing an insulin/zinc-induced hyperpolarization or a zinc-dependent blunting of an insulin-induced depolarization, Qiu *et al*. (2014) reported an insulin-induced depolarization. While it is unclear why the authors observed these apparent contradictory responses, we pursued a detailed investigation on the effects of zinc, zinc-containing, and zinc-free insulin on the activity of arcuate POMC neurons.

Analogous to the effects of zinc-containing insulin, zinc dose-dependently hyperpolarized arcuate POMC neurons. Although the chelating agent EDTA impaired the zinc-induced hyperpolarization by 75-fold, the inhibition of arcuate POMC neurons, induced by insulin, remained intact even after pretreatment with EDTA (Humulin-R or Sigma insulin). Moreover, zinc-free insulin hyperpolarized arcuate POMC neurons, supporting an insulin-dependent inhibition of arcuate POMC neurons. This might be less surprising given that the concentration of zinc-containing insulin commonly used to demonstrate the inhibition of arcuate POMC neurons (50 nM Humulin-R or Sigma insulin) contains amounts of zinc which were insufficient to alter membrane potential (Humulin-R: ~20 nM or Sigma insulin: ≤44 nM). Importantly, the effects of zinc-containing insulins (Humulin-R) and zinc-free insulin were abolished in POMC neurons deficient in for insulin receptors. These data are

consistent with previous reports demonstrating a requirement of insulin receptors and PI3K intracellular signalling in the inhibition of arcuate POMC neurons and other cell types induced by zinc-containing insulin (Spanswick *et al.*, 2000; Niswender *et al.*, 2003; Gelling *et al.*, 2006; Plum *et al.*, 2006; Hill *et al.*, 2008, 2010; Cotero and Routh, 2009; Klockener *et al.*, 2011; Huang *et al.*, 2018). These data also confirm that the concentration of zinc in commercially available mammalian insulin formulations, such as Humulin-R, is not sufficient to independently alter the activity of arcuate POMC neurons. Furthermore, chelation of zinc-containing insulin failed to blunt the hyperpolarization of arcuate NPY neurons. Together, these data support an insulin-induced inhibition of arcuate POMC and NPY neurons which is independent of zinc. Thus, the current study demonstrates that the zinc concentration (at the levels included in a variety of insulin formulations) was not sufficient to cause a change in POMC neuronal activity, alone.

Guinea pig insulin-induced depolarization of arcuate POMC neurons requires PDGF receptors and TRPC5 channel subunits, not insulin receptors or leptin receptors

In contrast to bovine and human insulin which bind zinc, guinea pig (hystricomorph) insulin exists as a monomeric species even in the presence of zinc (Zimmerman *et al.*, 1972, 1974; Zimmerman and Yip, 1974). Differences in physical properties between guinea pig and bovine/humulin insulin may contribute to differences in their metabolic activities (Zimmerman *et al.*, 1972, 1974; Zimmerman and Yip, 1974; King *et al.*, 1983; Chan *et al.*, 1984). Interestingly, hystricomorph insulins appear to exert these metabolic activities *via* a receptor that recognizes PDGF and not via insulin receptors (King *et al.*, 1983; Chan *et al.*, 1984). The differing trophic capabilities of guinea pig insulin may also have important relevance to the effects on the acute cellular activity of arcuate POMC neurons. In particular, guinea pig insulin depolarizes murine POMC neurons in the arcuate nucleus of hypothalamus, which is contrary to the effects of commonly used mammalian insulins. The activation of a non-selective cation conductance composed of TRPC5 channel subunits, induced by guinea pig insulin, was enriched in arcuate POMC neurons which express leptin receptors. Intriguingly, these data are analogous to recent work demonstrating that PDGF (which shares biological activity with guinea pig insulin; King *et al.*, 1983) activates a PLC-TRPC5/6-dependent mechanism in the midbrain of mice (Yao *et al.*, 2009). Moreover, POMC neurons express PDGF receptors and cognate signalling pathways (Henry *et al.*, 2015; Silva *et al.*, 2016; Campbell *et al.*, 2017). Importantly, TRPC5 channels are a common downstream target of both leptin and 5-HT_{2C} receptors in POMC neurons to regulate energy balance and glucose homoeostasis (Gao *et al.*, 2017). While both guinea pig insulin and leptin require TRPC5 channel subunits in the acute activation of arcuate POMC neurons, guinea pig insulin depolarized POMC neurons independent of both insulin receptors and leptin receptors. Rather, the activation of arcuate POMC neurons induced by guinea pig insulin, was blocked by PDGF receptor antagonism. Thus, guinea pig insulin activated murine POMC neurons by targeting cellular mechanisms shared with other metabolic regulators. However, this action was dependent upon putative PDGF receptors and not on insulin receptors and leptin receptors. The excitatory effect and the investigation of the cellular mechanism of guinea pig insulin on arcuate POMC neurons support a possible PDGF receptor-dependent mechanism in regulating the metabolism and energy balance in rodents. Together, these data may provide a new target for the treatment of metabolic disease.

In summary, guinea pig insulin acutely stimulated, while other mammalian insulin formulations inhibited, the activity of arcuate POMC neurons. The acute inhibitory effects of mammalian insulin formulations were independent of zinc and required insulin receptors. Conversely, guinea pig insulin depolarized arcuate POMC neurons *via* PDGF receptors and TRPC5 channel subunits, an effect that was independent of both insulin receptors and leptin receptors. These data highlight a previously recognized property of guinea pig insulin to mediate trophic effects through receptors different from other mammalian insulin receptors. Moreover, these data confirm that the acute effect of insulin in arcuate POMC neurons is predominantly inhibitory.

Acknowledgements

We thank Dr. Joel K. Elmquist (of the Division of Hypothalamic Research, Department of Internal Medicine, UT Southwestern Medical Center, Dallas, Texas) for kindly providing us with the *NPY*-hrGFP and POMC-hrGFP mice. We also thank Chad D. Paavola and Michael Akers of Eli Lilly for generously providing the zinc-free insulin. This work was supported by The Guangdong Provincial Clinical Medical Centre for Neurosurgery (no. 2013B020400005) and grants to K.W.W. from National Institute of Diabetes and Digestive and Kidney Diseases (nos R01 DK100699 and R01 DK119169).

Author contributions

K.W.W. conceived and designed the study. Z.Y.H. and Y.G. designed and performed all electrophysiology experiments, analysed the data and wrote the manuscript. L.L. and S.A. assisted performing experiments, analysed the data and wrote the manuscript. H.B.G. edited the manuscript.

Conflict of interest

The authors declare no conflicts of interest.

Declaration of transparency and scientific rigour

This Declaration acknowledges that this paper adheres to the principles for transparent reporting and scientific rigour of preclinical research recommended by funding agencies,

publishers and other organisations engaged with supporting research.

References

Alexander SPH, Fabbro D, Kelly E, Marrion NV, Peters JA, Faccenda E *et al*. (2017a). The Concise Guide to PHARMACOLOGY 2017/18: Catalytic receptors. Br J Pharmacol 174 : S225–S271.

Alexander SPH, Striessnig J, Kelly E, Marrion NV, Peters JA, Faccenda E *et al*. (2017b). The Concise Guide to PHARMACOLOGY 2017/18: Voltage-gated ion channels. Br J Pharmacol 174: S160–S194.

Alexander SP, Fabbro D, Kelly E, Marrion NV, Peters JA, Faccenda E *et al*. (2017c). The Concise Guide to PHARMACOLOGY 2017/18: Enzymes. Br J Pharmacol 174: S272–S359.

Alexander SPH, Christopoulos A, Davenport AP, Kelly E, Marrion NV, Peters JA *et al*. (2017d). The Concise Guide to PHARMACOLOGY 2017/18: G protein-coupled receptors. Br J Pharmacol 174: S17–S129.

Aponte Y, Atasoy D, Sternson SM (2011). AGRP neurons are sufficient to orchestrate feeding behavior rapidly and without training. Nat Neurosci 14: 351–355.

Balthasar N, Coppari R, McMinn J, Liu SM, Lee CE, Tang V*et al*. (2004). Leptin receptor signaling in POMC neurons is required for normal body weight homeostasis. Neuron 42: 983–991.

Berglund ED, Liu C, Sohn JW, Liu T, Kim MH, Lee CE *et al*. (2013). Serotonin 2C receptors in pro-opiomelanocortin neurons regulate energy and glucose homeostasis. J Clin Invest 123: 5061–5070.

Bruning JC, Gautam D, Burks DJ, Gillette J, Schubert M, Orban PC *et al*. (2000). Role of brain insulin receptor in control of body weight and reproduction. Science 289: 2122–2125.

Bruning JC, Michael MD, Winnay JN, Hayashi T, Horsch D, Accili D *et al*. (1998). A muscle-specific insulin receptor knockout exhibits features of the metabolic syndrome of NIDDM without altering glucose tolerance. Mol Cell 2: 559–569.

Campbell JN, Macosko EZ, Fenselau H, Pers TH, Lyubetskaya A, Tenen D *et al*. (2017). A molecular census of arcuate hypothalamus and median eminence cell types. Nat Neurosci 20: 484–496.

Chan SJ, Episkopou V, Zeitlin S, Karathanasis SK, MacKrell A, Steiner DF *et al*. (1984). Guinea pig preproinsulin gene: an evolutionary compromise? Proc Natl Acad Sci U S A 81: 5046–5050.

Cotero VE, Routh VH (2009). Insulin blunts the response of glucose-excited neurons in the ventrolateral-ventromedial hypothalamic nucleus to decreased glucose. Am J Physiol Endocrinol Metab 296: E1101–E1109.

Gao Y, Yao T, Deng Z, Sohn JW, Sun J, Huang Y*et al*. (2017). TrpC5 mediates acute leptin and serotonin effects via Pomc neurons. Cell Rep 18: 583–592.

Gelling RW, Morton GJ, Morrison CD, Niswender KD, Myers MG Jr, Rhodes CJ *et al*. (2006). Insulin action in the brain contributes to glucose lowering during insulin treatment of diabetes. Cell Metab 3: 67–73.

Harding SD, Sharman JL, Faccenda E, Southan C, Pawson AJ, Ireland S *et al*. (2018). The IUPHAR/BPS Guide to PHARMACOLOGY in 2018: updates and expansion to encompass the new guide to IMMUNOPHARMACOLOGY. Nucl Acids Res 46: D1091–D1106.

He Z, Gao Y, Alhadeff AL, Castorena C, Huang Y, Lieu L *et al*. (2018). Cellular and synaptic reorganization of arcuate NPY/AgRP and POMC neurons after exercise. Mol Metab 18: 107–119.

Henry FE, Sugino K, Tozer A, Branco T, Sternson SM (2015). Cell type-specific transcriptomics of hypothalamic energy-sensing neuron responses to weight-loss. Elife 4.

Hill JW, Elias CF, Fukuda M, Williams KW, Berglund ED, Holland WL *et al*. (2010). Direct insulin and leptin action on pro-opiomelanocortin neurons is required for normal glucose homeostasis and fertility. Cell Metab 11: 286–297.

Hill JW, Williams KW, Ye C, Luo J, Balthasar N, Coppari R *et al*. (2008). Acute effects of leptin require PI3K signaling in hypothalamic proopiomelanocortin neurons in mice. J Clin Invest 118: 1796–1805.

Huang Y, He Z, Gao Y, Lieu L, Yao T, Sun J *et al*. (2018). Phosphoinositide 3-kinase is integral for the acute activity of leptin and insulin in male arcuate NPY/AgRP neurons. J Endocr Soc 2: 518–532

Kilkenny C, Browne W, Cuthill IC, Emerson M, Altman DG, Group NCRRGW (2010). Animal research: reporting *in vivo* experiments: the ARRIVE guidelines. Br J Pharmacol 160: 1577–1579.

King GL, Kahn CR, Heldin CH (1983). Sharing of biological effect and receptors between guinea pig insulin and platelet-derived growth factor. Proc Natl Acad Sci U S A 80: 1308–1312.

Klockener T, Hess S, Belgardt BF, Paeger L, Verhagen LA, Husch A *et al*. (2011). High-fat feeding promotes obesity via insulin receptor/PI3K-dependent inhibition of SF-1 VMH neurons. Nat Neurosci 14: 911–918.

Krashes MJ, Koda S, Ye C, Rogan SC, Adams AC, Cusher DS *et al*. (2011). Rapid, reversible activation of AgRP neurons drives feeding behavior in mice. J Clin Invest 121: 1424–1428.

McGrath JC, Lilley E (2015). Implementing guidelines on reporting research using animals (ARRIVE etc.): new requirements for publication in BJP. Br J Pharmacol 172: 3189–3193.

Niswender KD, Morrison CD, Clegg DJ, Olson R, Baskin DG, Myers MG Jr *et al*. (2003). Insulin activation of phosphatidylinositol 3-kinase in the hypothalamic arcuate nucleus: a key mediator of insulin-induced anorexia. Diabetes 52: 227–231.

Plum L, Ma X, Hampel B, Balthasar N, Coppari R, Munzberg H *et al*. (2006). Enhanced PIP3 signaling in POMC neurons causes KATP channel activation and leads to diet-sensitive obesity. J Clin Invest 116: 1886–1901.

Plum L, Schubert M, Bruning JC (2005). The role of insulin receptor signaling in the brain. Trends Endocrinol Metab 16: 59–65.

Qiu J, Wagner EJ, Ronnekleiv OK, Kelly MJ (2018). Insulin and leptin excite anorexigenic pro-opiomelanocortin neurones via activation of TRPC5 channels. J Neuroendocrinol 30: e12501.

Qiu J, Zhang C, Borgquist A, Nestor CC, Smith AW, Bosch MA *et al*. (2014). Insulin excites anorexigenic proopiomelanocortin neurons via activation of canonical transient receptor potential channels. Cell Metab 19: 682–693.

Silva JP, Lambert G, van Booven D, Wahlestedt C (2016). Epigenomic and metabolic responses of hypothalamic POMC neurons to gestational nicotine exposure in adult offspring. Genome Med 8: 93.

Sohn JW, Williams KW (2012). Functional heterogeneity of arcuate nucleus pro-opiomelanocortin neurons: implications for diverging melanocortin pathways. Mol Neurobiol 45: 225–233.

Spanswick D, Smith MA, Mirshamsi S, Routh VH, Ashford ML (2000). Insulin activates ATP-sensitive K+ channels in hypothalamic neurons of lean, but not obese rats. Nat Neurosci 3: 757–758.

Steculorum SM, Ruud J, Karakasilioti I, Backes H, Engstrom Ruud L, Timper K *et al*. (2016). AgRP neurons control systemic insulin sensitivity via myostatin expression in brown adipose tissue. Cell 165: 125–138.

Sun J, Gao Y, Yao T, Huang Y, He Z, Kong X *et al*. (2016). Adiponectin potentiates the acute effects of leptin in arcuate *Pomc* neurons. Mol Metab 5: 882–891.

Williams KW, Liu T, Kong X, Fukuda M, Deng Y, Berglund ED *et al*. (2014). Xbp1s in Pomc neurons connects ER stress with energy balance and glucose homeostasis. Cell Metab 20: 471–482.

Williams KW, Margatho LO, Lee CE, Choi M, Lee S, Scott MM *et al*. (2010). Segregation of acute leptin and insulin effects in distinct populations of arcuate proopiomelanocortin neurons. J Neurosci 30: 2472–2479.

Woods SC, Lotter EC, McKay LD, Porte D Jr (1979). Chronic intracerebroventricular infusion of insulin reduces food intake and body weight of baboons. Nature 282: 503–505.

Xu J, Bartolome CL, Low CS, Yi X, Chien CH, Wang P *et al*. (2018). Genetic identification of leptin neural circuits in energy and glucose homeostases. Nature 556: 505–509.

Yao H, Peng F, Fan Y, Zhu X, Hu G, Buch SJ (2009). TRPC channel-mediated neuroprotection by PDGF involves Pyk2/ERK/CREB pathway. Cell Death Differ 16: 1681–1693.

Zimmerman AE, Kells DI, Yip CC (1972). Physical and biological properties of guinea pig insulin. Biochem Biophys Res Commun 46: 2127–2133.

Zimmerman AE, Moule ML, Yip CC (1974). Guinea pig insulin. II Biological activity. J Biol Chem 249: 4026–4029.

Zimmerman AE, Yip CC (1974). Guinea pig insulin. I Purification and physical properties. J Biol Chem 249: 4021–4025.

Supporting Information

Additional supporting information may be found online in the Supporting Information section at the end of the article.

https://doi.org/10.1111/bph.14559

Figure S1 Pretreatment of 450nM EDTA failed to block the leptin induced activation of POMC neurons. (A) A representative trace shows that pretreatment with EDTA (450nM) fails to block the leptin (100 nM) induced depolarization of POMC neurons. (B) Histogram illustrates the leptin-induced change in membrane potential of POMC neurons with the pretreatment of 450nM EDTA. Dotted line: treatment of EDTA. Error bars indicate SEM. (n = 10. Data from 4 mice).

Figure S2 Insulin hyperpolarizes arcuate NPY neurons independent of zinc. (A–D) Brightfield illumination (A) of an NPY neuron from NPY-hrGFP mice. (B) Shows the same neuron under FITC (hrGFP) illumination. Complete dialysis of Alexa Fluor 350 from the intracellular pipette is shown in (C) and merged image of targeted NPY neuron (D). Arrow indicates the targeted cell. Scale bar = 50 μm. (E&G) Representative traces depict that NPY neurons are hyperpolarized by Humulin-R (50 nM) and insulin (50 nM, Sigma). (F&H) Administration of EDTA fails to block either the Humulin-R (50 nM) or insulin (50 nM, Sigma; H) induced hyperpolarization of NPY neurons. (I) Histogram illustrates the insulin-induced changes in membrane potential of NPY neurons with or without EDTA. Error bars indicate SEM. (Humulin-R: n = 13; Humulin-R + EDTA: n = 8; Sigma-insulin: n = 7; Sigma-insulin+EDTA: n = 9. Data from 13 mice).

Figure S3 Pretreatment of PDGF receptor antagonist failed to block the insulin induced effect of POMC neurons. (A) A representative trace shows that pretreatment with PDGF receptor antagonist (100 nM CP 673451) fails to block the insulin (50 nM, Humulin-R, Eli Lilly) induced hyperpolarization of POMC neurons. (B) Histogram illustrates insulin-induced changes of membrane potential of POMC neurons with the pretreatment of 100nM CP 673451. Dotted line: treatment of CP 673451. Error bars indicate SEM. (n = 7. Data from 3 mice).

Figure S4 Guinea pig insulin hyperpolarized NPY neurons. (A) A representative trace shows that the guinea pig insulin (50nM) induced hyperpolarization of NPY neurons. (B) Histogram illustrates guinea pig insulin-induced change of membrane potential in NPY neurons. Error bars indicate SEM. (n = 10. Data from 4mice).

Figure S5 Pretreatment of PDGF receptor antagonist blocked the guinea pig insulin induced effect of NPY neurons. (A) A representative trace shows that pretreatment with PDGF receptor antagonist (100nM CP 673451) prevents the Guinea pig insulin (50 nM) induced hyperpolarization of NPY neurons. (B) Histogram illustrates Guinea pig insulin-induced change of membrane potential of NPY neurons with the pretreatment of 100nM CP 673451. Dotted line: treatment of CP 673451. Error bars indicate SEM. (n = 6. Data from 3 mice).

Figure S6 Schematic showing zinc-free insulin inhibits arcuate POMC neurons through insulin receptors and K_{ATP} channels, independent of Zinc. However, guinea pig insulin depolarizes POMC neurons *via* PDGF receptors and TRPC5 subunits, while independent of insulin or leptin receptors.